

皮秒激光两步扫描实现玻璃快速密封焊接

陈聪^{1,2}, 廖洋^{2*}, 郭向朝³, 崔新强³, 冯吉军¹, 郑凯², 刘科², 谢少明², 彭宇杰², 冷雨欣^{2**}¹上海理工大学光电信息与计算机工程学院上海市现代光学系统重点实验室, 上海 200093;²中国科学院上海光学精密机械研究所强场激光物理国家重点实验室, 上海 201800;³中国科学院上海光学精密机械研究所高功率激光单元技术实验室, 上海 201800

摘要 为实现石英玻璃的快速密封焊接, 本文提出了一种利用皮秒激光进行两步扫描的焊接方法, 首先利用较高能量脉冲快速扫描, 在玻璃界面形成初步焊接, 再利用较低能量脉冲慢速扫描, 扩大熔池体积。在焊接强度和密封性能等方面, 将两步扫描焊接与传统单步扫描焊接进行了对比, 结果表明: 两步扫描焊接样品具有更高的焊接强度(平均剪切强度达到了 45 MPa), 同时可实现更好的密封效果。为了探究不同间隙宽度下玻璃焊接强度的变化, 通过滴加含不同直径 SiO₂ 微球的分散液增大玻璃间隙, 结果发现两步扫描方法可以对间隙超过 27 μm 的石英玻璃进行一定强度的焊接(剪切强度为 2.4 MPa)。基于此方法, 成功实现了石英玻璃的高强度快速密封焊接, 并利用单一皮秒激光扫描平台演示了微通道的快速制备和封装。

关键词 激光技术; 玻璃连接; 密封焊接; 两步扫描; 微通道封装; 皮秒激光

中图分类号 TG456.7 **文献标志码** A

DOI: 10.3788/CJL230602

1 引言

玻璃具有良好的理化性质(如透光性好、硬度高、耐腐蚀等), 是现代工业生产中不可缺少的优良材料。近年来, 随着高端光电子器件和微流控芯片的快速发展, 经常需要对玻璃材料进行高精度连接, 而且对连接强度和密封性能都有着较高要求。传统的玻璃连接技术主要包括长脉冲激光焊接^[1-6]、胶合黏接^[7]和高温熔接等方法, 但这些方法连接的玻璃样品在连接处存在易引入杂质、不耐高温、寿命较短或形变较大等缺点。

超快激光聚焦后峰值功率密度极高, 通过非线性多光子吸收能够以较高的精度将能量沉积在透明介质内部。当超快激光聚焦在两片玻璃接触面附近时, 光致电离所产生的局部高温使聚焦区域附近的材料快速熔化和固化, 从而使材料焊接在一起^[8-11]。超快激光焊接具有精度高、强度高、热稳定性好等优点, 因此近年来受到了越来越多的关注。目前很多研究人员采用显微物镜聚焦进行焊接^[12], 取得了不错的效果, 但该方法对材料的表面平整度有较高要求, 而且需要利用夹具加压进行固定, 焊接速度较慢, 不能对较厚材料进行焊接, 从而大大限制了该技术的应用。2015年, 英国和德国的研究人员分别利用皮秒激光^[13]和“脉冲串”模式的飞秒激光^[14]获得了大尺寸熔池, 从而实现了非光学

接触玻璃之间的焊接(间隙约为 3 μm)。2018年, 国内学者利用贝塞尔光束进行大焦深焊接, 大幅提升了激光焦点的轴向容差范围。2019年, 多位学者采用振镜和 *F*-theta 透镜代替显微物镜和位移平台进行聚焦扫描, 大幅提高了扫描速度, 而且较长的瑞利长度降低了对焦难度^[15-17]。特别地, 研究人员采用皮秒激光结合振镜快速振荡扫描方法实现了自然堆叠玻璃的焊接(间隙约为 10 μm)^[16-17]。

尽管大体积熔池或热影响区可以实现大间隙焊接, 但热积累导致的残余应力易导致微裂纹产生, 尤其是当需要形成连续焊缝时, 开裂现象更容易发生, 增大了玻璃密封焊接的难度。为解决上述问题, 笔者提出了一种基于振镜长焦距快速扫描的皮秒激光玻璃密封焊接方法——两步扫描焊接(TSSW), 即: 先用较高的脉冲能量进行快速扫描, 在焊接界面形成初步焊接, 再用高重复频率、低能量激光脉冲进行慢速扫描, 扩大熔池体积。高能量激光脉冲扫描形成的初始焊缝中存在色心、微孔洞等缺陷, 这些缺陷作为种子点反过来会促进后续低能量脉冲的吸收。将大脉冲能量诱导多光子吸收和缺陷诱导光吸收分步进行, 有效缓解了热裂纹的产生。利用此方法, 笔者成功实现了自然堆叠玻璃的高强度快速密封焊接, 并利用单一皮秒激光扫描平台演示了微通道的快速制备和封装。

收稿日期: 2023-03-09; 收稿日期: 2023-03-29; 录用日期: 2023-04-12; 网络首发日期: 2023-04-23

基金项目: 国家重点研发计划(2022YFE0107400)、国家自然科学基金(11774235, 61705130, 11933005)、上海市科学技术委员会资助项目(23010503600)、上海市高校特聘教授(东方学者)岗位计划(GZ2020015)

通信作者: *superliao@siom.ac.cn; **lengyuxin@mail.siom.ac.cn

2 实验

2.1 实验材料与设备

实验中使用的材料为熔融石英玻璃,其几何尺寸为 $20\text{ mm} \times 20\text{ mm} \times 1\text{ mm}$,平面度优于 $\lambda/4$ 。实验中使用的红外皮秒激光器的参数如下:波长 1064 nm ,脉冲宽度 10 ps ,最大输出功率 60 W ,重复频率在 $100\sim 1500\text{ kHz}$ 范围内连续可调。此外,焊接装置还包括扩束镜、反射镜、扫描振镜、 F -theta 透镜和三维位移平台,如图 1 所示。其中:扫描振镜是北京世纪桑尼科技有限公司生产的 S-9320D 型振镜,透镜焦距为 100 mm ,聚焦光斑大小约为 $15\text{ }\mu\text{m}$;调控玻璃间隙使用的 SiO_2 微球购于清河县安迪金属材料有限公司;测量玻璃间隙采用的扫描电子显微镜 (SEM) 的型号为 ZEISS Gemini 300;测试样品剪切强度采用的是新三思 (深圳) 实验设备有限公司生产的 CMT5105 型微机控制电子万能试验机。

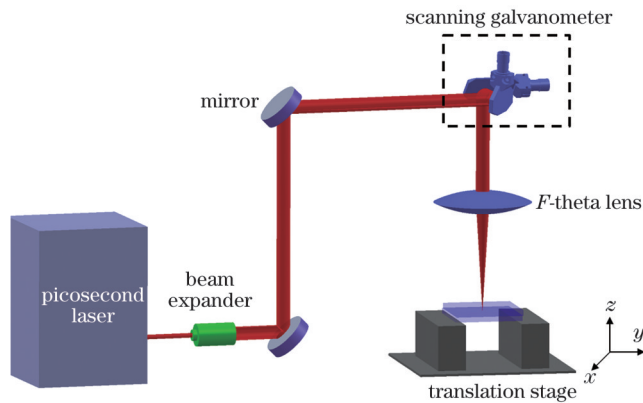


图 1 皮秒激光密封焊接装置

Fig. 1 Experimental set-up of picosecond laser seal welding

2.2 实验方法

利用两步扫描方式进行密封焊接,焊接步骤如下:

1) 在待焊接玻璃之间滴加少量无水乙醇或含不同直径 SiO_2 微球的乙醇分散液,以改变待焊接玻璃的间隙,其中分散液中 SiO_2 微球的含量较低,不会对焊接产生影响。

2) 设置重复频率为 $100\sim 300\text{ kHz}$,将激光束聚焦于玻璃的接触间隙,以 $200\sim 500\text{ mm/s}$ 的速度扫描;采用较高的脉冲能量,使皮秒激光在两片玻璃的接触面附近诱导产生多光子吸收,形成少量色心或微孔洞等缺陷。

3) 将重复频率改为 $1000\sim 1500\text{ kHz}$,以 $20\sim 50\text{ mm/s}$ 的速度沿原路径扫描多次,利用步骤 2) 形成的焊缝增强激光吸收,扩大熔池体积,熔融材料冷却后填充大尺度焊缝。

通过研究不同焊接参数的影响得出皮秒激光参数、焊缝间距、扫描速度、扫描次数的最佳值,实现玻璃的快速密封焊接。

图 2 给出了两步扫描焊接示意图。首先用高脉冲

能量、低重复频率的皮秒脉冲快速扫描,在焊接界面上进行初步焊接,形成较小的焊接熔池,如图 2(a) 和图 2(c) 所示;然后采用低脉冲能量、高重复频率激光脉冲进行慢速扫描,利用多脉冲作用产生的热效应扩大熔池体积,如图 2(b) 和图 2(d) 所示。

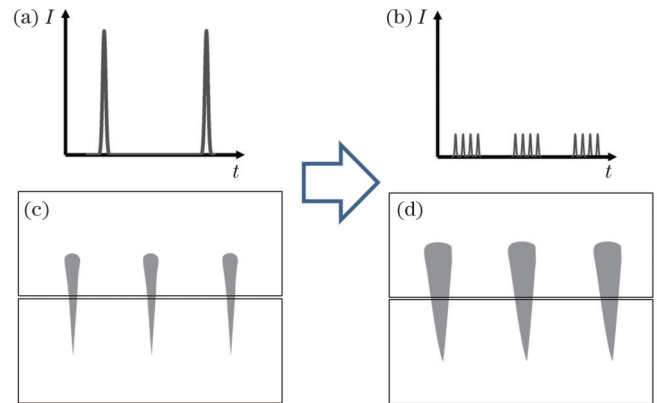


图 2 两步扫描焊接示意图。(a) 第一步扫描采用的激光脉冲序列;(b) 第二步扫描采用的激光脉冲序列;(c) 第一步扫描后形成的小尺寸焊接熔池;(d) 第二步扫描后形成的大尺寸焊接熔池

Fig. 2 Schematic diagrams of the two-step scanning welding strategy. (a) Laser pulse sequences for the first scanning welding; (b) laser pulse sequences for the second scanning welding; (c) small welding pool achieved by the first scanning; (d) large welding pool achieved by the second scanning

3 分析与讨论

为了观察两步扫描焊接相比于单步扫描焊接 (SSSW) 的优势,进行了单步扫描焊接和两步扫描焊接对照实验。单步扫描焊接参数为:激光脉冲能量 $50\text{ }\mu\text{J}$,重复频率 200 kHz ,扫描速度 200 mm/s ,重复扫描 10 次。对于两步扫描焊接,第一步所用参数与单步扫描焊接参数相同,且为单次扫描;第二步扫描参数为:激光脉冲能量 $8.3\text{ }\mu\text{J}$,重复频率 1200 kHz ,扫描速度 40 mm/s ,重复扫描 10 次。其中,单步扫描产生的总辐照剂量为 29.3 J/mm^2 ,两步扫描产生的总辐照剂量为 149.3 J/mm^2 ,约为单步扫描的 5 倍。由于单步扫描的单脉冲能量较高,辐照剂量过大时材料开裂严重,导致焊接质量迅速下降,所以实验中采用低脉冲能量多次扫描的方法增加熔池体积。两种方法焊接前,样品均处于没有加微球的自然堆叠状态,焊接后得到的焊缝截面如图 3 所示。从光学显微图可以看出,相比于单步扫描,两步扫描时的焊缝宽度明显更大,玻璃间隙被填充的范围更大。选取图 3 中的 9 条焊缝进行测量,得出单步扫描焊缝宽度的平均值为 $39\text{ }\mu\text{m}$,两步扫描焊缝宽度的平均值为 $56\text{ }\mu\text{m}$,这表明两步扫描焊接确实有增大熔池的效果。

采用万能试验机对单步扫描焊接和两步扫描焊接样品进行焊接强度测试。分别采用两种方法在同样条

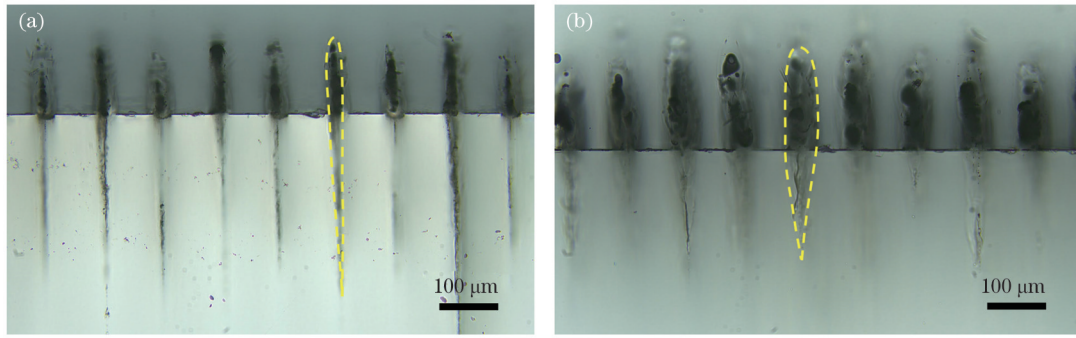


图 3 不同焊接方法获得的焊缝截面的透射光学显微图。(a)单步扫描;(b)两步扫描

Fig. 3 Transmission optical microscopy images of the welding cross sections obtained with different welding methods. (a) Single-step scanning welding (SSSW); (b) two-step scanning welding (TSSW)

件下重复焊接了 5 个样品,对每个样品的剪切强度进行测试,测试结果如图 4 所示,其中单步扫描焊接样品 2 在测试中脱落,没有有效数据。实验结果表明,虽然两种方法焊接的样品的强度测试结果均有一定波动,但两步扫描焊接样品的剪切强度显著高于单步扫描焊接样品,两步扫描焊接样品的平均剪切强度达到了 45 MPa。由于焊接强度极易受玻璃内部裂纹的影响,因此较高剪切强度的获得不仅归因于二次焊接后熔池的增大,也归因于较低的脉冲能量扫描有效缓解了热裂纹的产生。

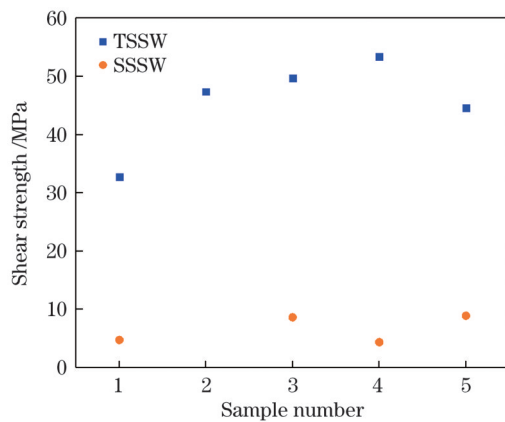


图 4 单步扫描焊接和两步扫描焊接样品的剪切强度测试结果
Fig. 4 Shear strength test results of welded samples by SSSW and TSSW

一般来说,玻璃间隙越大,焊缝的填充和连接越困难。为了探究两步扫描焊接方法所能够填充的最大间隙,焊接前在玻璃之间滴加含有不同直径 SiO₂ 微球的乙醇分散液。在实际操作中,玻璃间隙中的 SiO₂ 微球可能产生堆叠,使实际间隙大于微球直径,因此在焊接后使用扫描电子显微镜(SEM)测试了实际间隙。由于在焊接过程中没有加压,间隙存在一定的不一致性,图 5(b) 中的间隙宽度是对焊接后样品进行测量的结果;用扫描电镜(SEM)测量焊接后样品的间隙宽度,每个样品选取三个不同位置进行测量后取平均值。图 5(a) 是采用扫描电镜测量间隙宽度过程中选取的位置之一,其对应的间隙宽度为 16.5 μm。图 5(b) 给出了不同间隙下两步扫描焊接样品的剪切强度测试结果,可以看出:两步扫描焊接方法可以对间隙超过 27 μm 的石英玻璃进行一定强度的焊接(剪切强度为 2.4 MPa);随着玻璃间隙增大,焊接强度显著降低。

图 6 展示了单步扫描焊接和两步扫描焊接样品的水密封测试对比,扫描路径为封闭的同心圆,外径为 16 mm,内径为 15.2 mm,焊接前样品处于没有加微球的自然堆叠状态。可以看出焊接后两样品表面都出现了明显的干涉条纹,这是焊接后玻璃的间隙缩小后产生的白光干涉现象^[17],如图 6(a)和图 6(b)所示。其中,两步扫描焊接样品的干涉条纹沿焊缝出现了明显的边

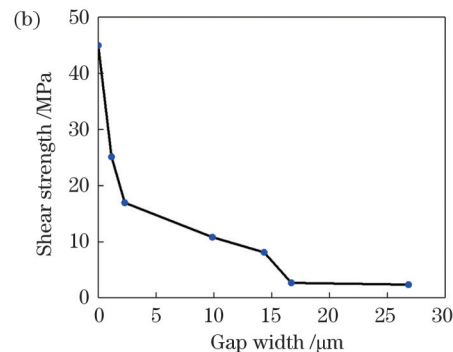
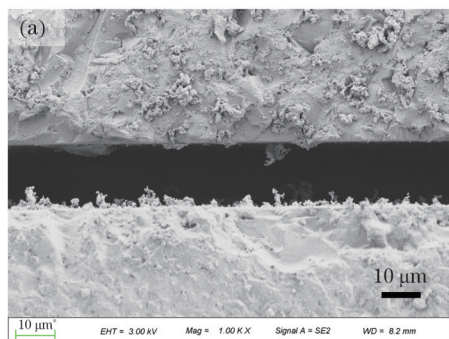


图 5 玻璃间隙的 SEM 测量结果以及两步扫描焊接样品的剪切强度随间隙宽度的变化。(a)玻璃间隙的 SEM 测量结果;(b)剪切强度随间隙宽度的变化

Fig. 5 SEM measurement result of the glass gap and variation of shear strengths of TSSW samples with gap width. (a) SEM measurement result of the glass gap; (b) variation of shear strength with gap width

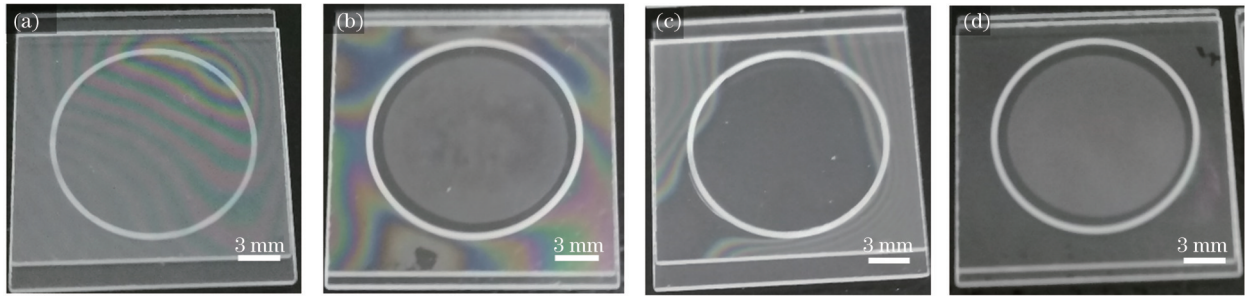


图 6 单步扫描焊接和两步扫描焊接样品的水密封测试对比。(a)沿同心圆路径单步扫描焊接的样品;(b)沿同心圆路径两步扫描焊接的样品;(c)单步扫描焊接样品浸没水中一周后;(d)两步扫描焊接样品浸没水中一周后

Fig. 6 Water seal test for SSSW and TSSW samples. (a) An SSSW sample using the concentric-circle scan path; (b) a TSSW sample using the concentric-circle scan path; (c) SSSW samples after immersing in water for one week; (d) TSSW samples after immersing in water for one week

界,而单步扫描焊接样品的干涉条纹出现了不规则分布,这证明两步扫描焊接样品的焊缝具有更高的均匀性。浸没水中一周后,单步扫描焊接样品的圆形焊缝内部原有的干涉条纹消失,这表明水渗入到圆形焊缝中间区域,如图 6(c)所示;而两步扫描焊接样品在水中浸泡前后中间区域无明显变化,这表明水没有渗入到圆形焊缝中间区域,如图 6(d)所示。可见,两步扫描焊接不仅能实现均匀的焊缝,而且焊缝密封稳定性良好。

采用单步扫描焊接时,如果脉冲能量过低,激光的峰值功率密度可能低于多光子吸收的阈值,不能实现有效焊接;如果脉冲能量过大,在高脉冲能量作用下激光等离子体产生的温度梯度和冲击波容易导致裂纹产生,因此难以获得较好的密封性能。两步扫描焊接可以有效解决这一难题,即:先用高能量脉冲在焊接界面形成初始焊缝,再利用高重复频率的低能量脉冲扩大熔池体积,初始形成的焊缝中包含了色心、微孔洞等缺

陷,这些缺陷作为种子点反过来会促进后续低能量脉冲的吸收。两步扫描焊接将大能量脉冲诱导多光子吸收和缺陷诱导光吸收分步进行,在获得大体积熔池的同时有效缓解了热裂纹的产生。

为了验证利用两步扫描焊接进行微通道封装的可行性,按图 7 所示步骤完成了一个微通道的制备和封装,其中通孔、微槽的制备和封装焊接均采用同一套装置完成。首先在玻璃上用激光钻孔制造两个通孔(脉冲能量 $50 \mu\text{J}$,重复频率 200 kHz ,扫描速度 200 mm/s ,通孔直径 1 mm ,耗时 4 min),如图 7(a)所示;然后在两个通孔之间加工一个微槽(激光脉冲能量 $50 \mu\text{J}$,重复频率 200 kHz ,扫描速度 200 mm/s ,微槽宽度 $100 \mu\text{m}$,长度 10 mm ,深度小于 $10 \mu\text{m}$,耗时 1 s),如图 7(b)所示;最后盖上另一片玻璃,使两片玻璃处于自然堆叠状态,采用两步扫描焊接方法,围绕通孔和微槽进行密封焊接,耗时少于 6 min ,如图 7(c)所示。

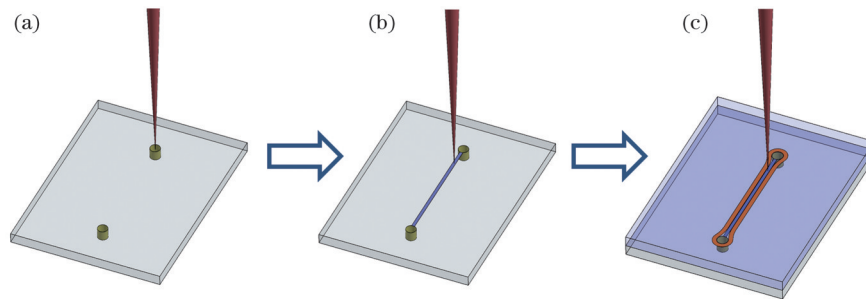


图 7 微通道制备示意图。(a)用激光在玻璃上加工通孔;(b)在通孔之间加工微槽;(c)沿通道边缘焊接密封

Fig. 7 Schematic diagram of microchannel preparation. (a) Drilling through-holes in the glass using laser; (b) machining a microgroove between through-holes; (c) seal welding along the microgroove edge

图 8 展示了按照上述步骤制备的微通道样品。为了检测其密封性,在一侧通孔中滴入罗丹明-B 染色液,染色液通过毛细作用在微通道中迅速渗透到另一侧通孔,可以清晰地看到染色液被限制在焊缝内围,表明微通道样品密封良好。

4 结 论

提出了一种基于振镜长焦距快速扫描的皮秒激光两

步扫描焊接方法:先用较高能量脉冲快速扫描,在焊接界面形成初步焊接,再通过高重复频率低能量激光脉冲慢速扫描,扩大熔池体积。实验结果表明,对于自然堆叠的两片石英玻璃,该方法既实现了较高的焊接强度,又实现了良好的密封性能,焊接后玻璃的平均剪切强度达到了 45 MPa ,焊接一周后仍能保持密封。通过在间隙中添加不同直径的 SiO_2 微球,探究了不同间隙下玻璃焊接强度的变化,结果发现两步扫描方法可以对间隙超过 $27 \mu\text{m}$

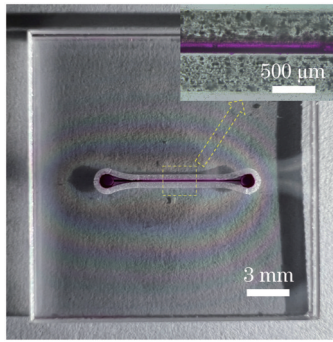


图 8 两步扫描焊接封装后的微通道样品

Fig. 8 A microchannel sample sealed by TSSW

的石英玻璃实现一定强度(剪切强度 2.4 MPa)的焊接。基于此方法,利用单一皮秒激光扫描平台实现了微通道的快速制备和封装,整体用时少于 10 min。

该方法将大能量脉冲诱导非线性多光子吸收和高重复频率小能量脉冲扩大熔池相结合,缓解了玻璃内部热裂纹的产生,在光电子器件、光学元件、微流控芯片连接和封装领域具有广阔的应用前景。

参 考 文 献

- [1] Luo C, Lin L W. The application of nanosecond-pulsed laser welding technology in MEMS packaging with a shadow mask[J]. *Sensors and Actuators A: Physical*, 2002, 97/98: 398-404.
- [2] Wu Q, Lorenz N, Cannon K M, et al. Glass frit as a hermetic joining layer in laser based joining of miniature devices[J]. *IEEE Transactions on Components and Packaging Technologies*, 2010, 33(2): 470-477.
- [3] Lin C Y, Shen Y H, Huang C C, et al. Laser sealing of organic light-emitting diode using low melting temperature glass frit[J]. *Optical and Quantum Electronics*, 2017, 49(6): 208.
- [4] Mescheder U M, Alavi M, Hiltmann K, et al. Local laser bonding for low temperature budget[J]. *Sensors and Actuators A: Physical*, 2002, 97/98: 422-427.
- [5] de Pablos-Martín A, Tismer S, Naumann F, et al. Evaluation of the bond quality of laser-joined sapphire wafers using a fresnoite-glass sealant[J]. *Microsystem Technologies*, 2016, 22(1): 207-214.
- [6] 陈根余, 钟沛新, 程少祥. 玻璃激光焊接过程中玻璃料与基板的耦合行为[J]. *中国激光*, 2021, 48(18): 1802005.
- [7] Chen G Y, Zhong P X, Cheng S X. Coupling behavior between glass frit and plate during laser-assisted glass frit bonding[J]. *Chinese Journal of Lasers*, 2021, 48(18): 1802005.
- [8] Pan Y J, Yang R J. A glass microfluidic chip adhesive bonding method at room temperature[J]. *Journal of Micromechanics and Microengineering*, 2006, 16(12): 2666-2672.
- [9] Takayuki T A M A K I, Wataru W A T A N A B E, Junji N I S H I I, et al. Welding of transparent materials using femtosecond laser pulses[J]. *Japanese Journal of Applied Physics*, 2005, 44(20/23): L687-L689.
- [10] Tamaki T, Watanabe W, Itoh K. Laser micro-welding of transparent materials by a localized heat accumulation effect using a femtosecond fiber laser at 1558 nm[J]. *Optics Express*, 2006, 14(22): 10460-10468.
- [11] 李鑫, 张彤, 季凌飞, 等. 皮秒激光扫描硅材料微孔自成形行为及机理研究[J]. *激光与光电子学进展*, 2022, 59(1): 0114005.
- [12] Li X, Zhang T, Ji L F, et al. Study on self-forming behavior and mechanism of picosecond laser scanning micropores in silicon materials[J]. *Laser & Optoelectronics Progress*, 2022, 59(1): 0114005.
- [13] 邹贵生, 林路禅, 肖宇, 等. 超快激光纳米连接及其在微纳器件制造中的应用[J]. *中国激光*, 2021, 48(15): 1502001.
- [14] Zou G S, Lin L C, Xiao Y, et al. Ultrafast laser nanojoining and its applications in the manufacturing of micro-nano devices[J]. *Chinese Journal of Lasers*, 2021, 48(15): 1502001.
- [15] Richter S, Döring S, Peschel T, et al. Breaking stress of glass welded with femtosecond laser pulses at high repetition rates[J]. *Proceedings of SPIE*, 2011, 7925: 79250P.
- [16] Chen J Y, Carter R M, Thomson R R, et al. Avoiding the requirement for pre-existing optical contact during picosecond laser glass-to-glass welding[J]. *Optics Express*, 2015, 23(14): 18645-18657.
- [17] Richter S, Zimmermann F, Eberhardt R, et al. Toward laser welding of glasses without optical contacting[J]. *Applied Physics A*, 2015, 121(1): 1-9.
- [18] Gstalter M, Chabrol G, Bahouka A, et al. Long focal length high repetition rate femtosecond laser glass welding[J]. *Applied Optics*, 2019, 58(32): 8858-8864.
- [19] Chen H, Deng L M, Duan J, et al. Picosecond laser welding of glasses with a large gap by a rapid oscillating scan[J]. *Optics Letters*, 2019, 44(10): 2570-2573.
- [20] Chen H, Duan J, Yang Z Q, et al. Picosecond laser seal welding of glasses with a large gap[J]. *Optics Express*, 2019, 27(21): 30297-30307.

Rapid Picosecond Laser Seal Welding of Glass Using a Two-Step Scanning Strategy

Chen Cong^{1,2}, Liao Yang^{2*}, Guo Xiangzhao³, Cui XinQiang³, Feng Jijun¹, Zheng Kai², Liu Ke², Xie Shaomin², Peng Yujie², Leng Yuxin^{2**}

¹Shanghai Key Laboratory of Modern Optical System, School of Optical-Electrical and Computer Engineering, University of Shanghai for Science and Technology, Shanghai 200093, China;

²State Key Laboratory of High Field Laser Physics, Shanghai Institute of Optics and Fine Mechanics, Chinese Academy of Sciences, Shanghai 201800, China;

³Key Laboratory of Materials for High Power Laser, Shanghai Institute of Optics and Fine Mechanics, Chinese Academy of Sciences, Shanghai 201800, China

Abstract

Objective In recent years, the high-precision sealing welding of glass materials has attracted wide attention because of its potential

applications in high-end optoelectronic devices and microfluidic chips. Traditional glass-joining methods typically utilize adhesives, which lead to limitations in high-temperature resistance, bonding strength, and durability. When nonlinear absorption at the interface is used between two materials, ultrafast laser welding offers several advantages, including high accuracy, high strength, and good thermal stability. However, achieving high strength and good sealing with high throughput remains challenging. In this study, we propose a picosecond laser sealing welding method based on two-step galvanometer scanning.

Methods Fused silica glass pieces with a thickness of 1 mm were used as welding materials. An infrared picosecond laser emitting a laser beam with a wavelength of 1064 nm was guided into a galvanometer scanner and focused using an F -theta lens with a focal distance of 100 mm. The welding process included the following four steps: 1) a small amount of ethanol or ethanol dispersion containing SiO_2 microspheres with different diameters was added into the glass gap to change the gap between the two glass pieces; 2) the laser pulses were set at a high pulse energy and a repetition rate of 100–300 kHz, and the laser beam focused at the joining interface was used to scan the glass pieces at a high speed of 200–500 mm/s; 3) the laser pulses were set at a low pulse energy and a repetition rate of 1000–1500 kHz, and multiple repeated scans were performed along the original path at a low speed of 20–50 mm/s; 4) the effects of various processing parameters on the two-step scanning welding, such as picosecond laser parameters, weld spacing, scanning speed, and scanning times, were investigated.

Results and Discussions For picosecond laser glass welding with a long focal length scan lens, one challenge is to reduce the thermal cracks caused by laser irradiation. However, the laser pulse energy must be sufficiently high to induce multiphoton absorption at the glass interface. To address this issue, fast scans relative to glass pieces with a high pulse energy were first performed to produce the initial welding microstructures at the joining interface, and then slow scans with a low pulse energy were conducted to enlarge the weld pool. To demonstrate the advantages of two-step scanning welding, several comparative experiments were performed between single-step scanning welding with a fixed pulse energy and two-step scanning welding with different pulse energies. Measurement results with optical microscopy show that the average weld joint widths by single- and two-step scanning are approximately 39 μm and 56 μm , respectively, revealing that two-step scanning welding can effectively enlarge the weld pool (Fig. 3). However, the average shear strength of two-step scanning welding reaches 45 MPa, which is significantly higher than that of single-step scanning welding under a high pulse energy. The higher shear strength of two-step scanning welding could be attributed not only to the enlargement of the weld pool by secondary welding but also to the reduction or fusion of thermal cracking by lower pulse energy scanning (Fig. 4). To explore the effects of the gap width between the two glass pieces on the welding strength, a small amount of ethanol dispersion containing SiO_2 microspheres of different diameters was added to the glass gap. The results show that the glass pieces with a gap of 27 μm can be joined with a shear strength of ~ 2.4 MPa using two-step scanning welding, and the welding strength decreases with an increase in the gap width (Fig. 5). To check the sealing performance, the welded samples were immersed in water for one week. For the sample obtained by single-step scanning welding, the original interference fringes inside the ring-shaped weld joint disappear, indicating that water penetrates the middle region through the weld joint. However, for the sample prepared by two-step scanning welding, no significant change was observed in the middle region of the ring-shaped weld joint after immersion. It can be deduced that two-step scanning welding not only achieves uniform and continuous welding but also has good sealing stability (Fig. 6). To demonstrate the potential application of two-step scanning welding in microchannel packaging, an open microgroove fabricated by picosecond laser ablation in a single glass piece was sealed with another glass piece through fast scanning welding. It can be clearly seen that the dye solution is confined within the weld joint (Figs. 7 and 8).

Conclusions To achieve rapid glass seal welding, a two-step picosecond laser scanning strategy was proposed by combining fast and slow scanning approaches with high and low pulse energies, respectively. For two naturally stacked fused silica pieces, the welding strength and sealing performance of the sample prepared by the two-step scanning strategy with two different pulse energies were demonstrated to be better than those of the sample prepared by the conventional single-step scanning process with a fixed pulse energy. Based on this technique, rapid preparation of a packaged microchannel was successfully realized using picosecond laser scanning. This technique combines nonlinear multiphoton absorption induced by high-energy laser pulses and molten pool enlargement derived from low-energy and high-repetition-rate laser pulses. The technique can effectively alleviate the generation of thermal cracks in the glass welding process and has broad applications in the connection and packaging fields of optoelectronic devices, optical components, and microfluidic chips.

Key words laser technique; glass joining; seal welding; two-step scanning; microchannel packaging; picosecond laser